



Cite this: *Energy Environ. Sci.*,  
2023, **16**, 3002

## Dimethyl ether/CO<sub>2</sub> – a hitherto underestimated H<sub>2</sub> storage cycle†

P. Schühle,<sup>a</sup> R. Stöber,<sup>a</sup> M. Semmel,<sup>d</sup> A. Schaadt,<sup>d</sup> R. Szolak,<sup>d</sup> S. Thill,<sup>c</sup> M. Alders,<sup>c</sup> C. Hebling,<sup>d</sup> P. Wasserscheid<sup>†abc</sup> and O. Salem<sup>\*d</sup>

Large amounts of renewable energy will have to be stored and transported in the future. For this task, chemical hydrogen storage technologies are particularly suitable. In this paper, we show that the DME/CO<sub>2</sub> storage cycle is especially promising for point-to-point transport of renewable hydrogen over long distances. Surprisingly, this technology has been neglected so far, as DME has been mostly discussed as a fuel substitute for internal combustion engines while the back transport of CO<sub>2</sub> has not been considered in this context. Our study reveals that the similarity of the physico-chemical properties of DME and CO<sub>2</sub> enables back-shipping of CO<sub>2</sub> after hydrogen release in the same vessel that is used to transport DME. This leads to an overall technology that shows in our analysis considerable potential to outperform ammonia or methanol, which are intensively discussed as hydrogen vectors today. The proposed cycle is characterised in particular by comparatively high energy efficiency, reduced mass flows per ton of delivered hydrogen, lower water consumption at the hydrogen production site and lower toxicological risks.

Received 22nd January 2023,  
Accepted 25th May 2023

DOI: 10.1039/d3ee00228d

rsc.li/ees

### Broader context

In this work, we introduce an innovative approach to renewable hydrogen transportation that could significantly impact a future global hydrogen economy. We've known for some time that hydrogen, specifically 'green' hydrogen, holds great promise as a carrier of clean energy. However, challenges in storing and transporting this elusive energy carrier have remained. To tackle these hurdles, our research team has cast new light on existing commodities: We propose the dimethyl ether (DME)/CO<sub>2</sub> storage cycle as a potential game-changer for long-range, point-to-point hydrogen transport. DME is used as hydrogen carrier, while the CO<sub>2</sub>, the coupling product of releasing hydrogen at the destination, is concurrently transported back in the same vessel for sustainable reuse. This method outperforms current frontrunners like ammonia and methanol on key metrics, delivering impressive advantages in energy efficiency, mass flows, water consumption, and toxicological risk reduction. By effectively addressing one of the most significant barriers to global hydrogen transportation, we hope that our findings will ignite further research and innovation toward cost-effective global hydrogen trading for a fully defossilized energy system around the globe.

## Introduction

Green molecules in the form of renewable hydrogen and hydrogen-based energy carriers will play a key role in the defossilisation of the global energy system. Green energy

molecules complement the ongoing expansion of renewable electricity and provide solutions for applications that are hard to electrify, such as seasonal energy storage, global energy trading, aviation, ship and heavy-duty mobility, and industrial applications.<sup>1,2</sup>

The promise of hydrogen lies in its versatility. It has equally the potential to be used as a combustion fuel (similar to natural gas) and for electricity generation using fuel cells, engines or turbines.<sup>1,3,4</sup> Moreover, hydrogen is a vital feedstock for a range of industries that produce chemicals and materials, today and in the future. For example, hydrogen is probably the only way to defossilise the hard-to-abate steel industry, where it will be used as a reducing agent and heat source for blast furnaces in the production.<sup>5,6</sup> In most electrochemical conversion, combustion and production scenarios, the oxidation of hydrogen provides CO<sub>2</sub>-emission free energy.

<sup>a</sup> Lehrstuhl für Chemische Reaktionstechnik, Friedrich-Alexander-Universität Erlangen-Nürnberg, Egerlandstr. 3, 91058 Erlangen, Germany

<sup>b</sup> Forschungszentrum Jülich, Helmholtz-Institute Erlangen-Nürnberg for Renewable Energy (IEK 11), Egerlandstr. 3, 91058 Erlangen, Germany.

E-mail: p.wasserscheid@fz-juelich.de

<sup>c</sup> Forschungszentrum Jülich, Institute for a Sustainable Hydrogen Economy, Am Brainenergy Park 4, 52428 Jülich, Germany

<sup>d</sup> Fraunhofer-Institute for Solar Energy Systems ISE, Heidenhofstr. 2, 79110 Freiburg, Germany. E-mail: ouda.salem@ise.fraunhofer.de

† Electronic supplementary information (ESI) available. See DOI: <https://doi.org/10.1039/d3ee00228d>



The extended use of hydrogen in the future energy and chemical sectors can only contribute to sustainability goals if it is produced in CO<sub>2</sub>-emission lean ways. In contrast, almost the complete current hydrogen production worldwide of more than 90 Mtpa,<sup>7</sup> is obtained from methane steam reforming<sup>8</sup> or coal gasification,<sup>9</sup> making hydrogen production responsible for over 2% of the global CO<sub>2</sub> emissions.<sup>7,10</sup> Measures to reduce CO<sub>2</sub> emissions in fossil-based hydrogen production include carbon capture and storage processes.<sup>11</sup> By using absorption and adsorption technologies, CO<sub>2</sub> can be isolated from the hydrogen product stream, to store it either in the form of CO<sub>2</sub> (blue hydrogen<sup>12</sup>) or in form of elemental carbon (turquoise hydrogen<sup>13</sup>) underground. Hydrogen production pathways that do not rely on fossil resources are summarized under the term 'green hydrogen'. There is a wide consensus that the most important source of 'green hydrogen' will be the electrolysis of water using renewable electricity from wind, sun and hydropower.<sup>14–16</sup> Whether this term covers hydrogen production from biomass is a matter of ongoing regulatory discussions.<sup>17</sup>

Hydrogen production from electrolysis is strongly dependent on electricity cost. For approximate calculations one can estimate that  $\frac{3}{4}$  of the hydrogen production cost results from the electricity price and  $\frac{1}{4}$  from the capital investment into the electrolyzer itself.<sup>18</sup> Roughly, 50 kW h of electricity are needed for producing 1 kg of hydrogen.<sup>19</sup> Consequently, the production of green hydrogen from water electrolysis is economically attractive where renewable electricity is available at low cost. This prerequisite is given at locations where sun, wind or hydropower are abundant and competing electricity demands are scarce, *e.g.* in areas with low density of population and/or low density of industrial activity. Consequently, the locations for future large-scale electrolysis operations will in most cases not coincide with the hydrogen consumption sites. Therefore, transportation, storage and on-demand supply of green hydrogen will develop into a decisive factor for the future success of a global hydrogen economy.

A particularly interesting topic is the long-range transportation of hydrogen or hydrogen-based energy carriers, *i.e.* transportation over more than 6.000 km (*e.g.* Perth–Rotterdam; Cape Town–Rotterdam, Patagonia–Rotterdam) as for such distances alternative energy transport options *via* electric grids or hydrogen pipelines are out of range. For such long-range transport scenarios of hydrogen, a number of important studies and papers have been published recently.<sup>20–24</sup> Due to the low volumetric energy density of gaseous compressed hydrogen, most of them consider ammonia (NH<sub>3</sub>), methanol (CH<sub>3</sub>OH), various liquid organic hydrogen carrier (LOHC) systems and cryogenic hydrogen as obvious transport options and include conversion, storage, shipping, and reconversion scenarios and the related cost. From the published results it is obvious, that the named transport options vary across technology readiness, energy conversion efficiency, infrastructure requirements and potential application scenarios.<sup>25,26</sup> Typically, quantitative key performance indicators, as well as qualitative aspects are considered to assess the different transport options in given

application scenarios. While some individual results vary depending on the technologies and assumptions, an important joint outcome of all these studies is that long transport distances are not an economic showstopper for future global green hydrogen logistics. The available studies state different advantages and disadvantages of individual technologies and thus identify room for new and better solutions. None of the so far discussed technologies provides an ideal solution for the overall challenge of global long-distance hydrogen transportation.

According to current forecasts based on hydrogen export projects under development, 12 Mt of hydrogen are expected to be traded globally by 2030, with 2.6 Mtpa planned to come online by 2026.<sup>7</sup> Electrolytic hydrogen production with ammonia as the carrier account for a major part of the announced projects while much smaller volumes are planned for synthetic liquid fuels, LOHC, liquefied hydrogen or compressed hydrogen by ship. Projects accounting for 40% of planned export volumes by 2030 have not yet identified a carrier molecule.<sup>7</sup>

## Dimethyl ether as hydrogen vector

This contribution highlights the potential of dimethyl ether (DME) as alternative future hydrogen vector. For long-range hydrogen transport scenarios, a high hydrogen storage capacity of the applied hydrogen vector is crucial for economic success. Our consideration starts with a general remark on how these hydrogen storage capacities have been calculated so far. As found in many publications on the comparison of different hydrogen storage molecules,<sup>25,27,28</sup> the traditional way to determine the hydrogen capacity of a hydrogen carrier molecule is to simply relate the weight of its releasable hydrogen to its total weight:

$$w_{H_2, \text{carrier}} = \frac{m_{H_2, \text{carrier}}}{m_{\text{carrier}}} \quad (1)$$

However, the example of methanol shows impressively (see eqn (3)), that this is a simplified and to some extend misleading way to evaluate the technical hydrogen storage capacity of a carrier. Methanol can be generated by CO<sub>2</sub> hydrogenation at energy-rich locations. During hydrogen release at the place of energy demand, not only the hydrogen bound to methanol is provided. Additionally, the technically applied steam reforming process generates one extra mol of hydrogen per mol of methanol from added water. Regarding hydrogen logistics, this water is not transported but it is already available at the location of hydrogen and energy demand. Considering this effect, we propose the calculation of a technical hydrogen capacity of hydrogen carrier molecules, by simply comparing the weight of released hydrogen with the weight of the transported hydrogen carrier:

$$w_{H_2, \text{technical}} = \frac{m_{H_2, \text{released}}}{m_{\text{carrier}}} \quad (2)$$

Doing so, we find that the technical hydrogen capacity of methanol is 18.8 wt% instead of 12.5 wt%, as calculated from the hydrogen weight in methanol and typically stated in the



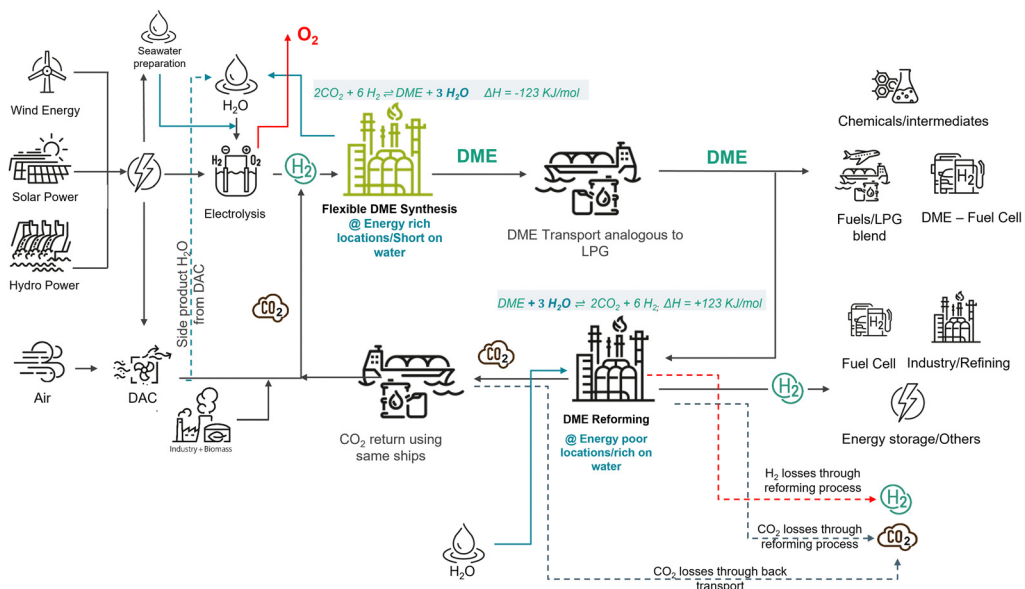


Fig. 1 DME value chain if used as a global H<sub>2</sub> carrier.

available literature on hydrogen transport options.<sup>29,30</sup> Thus, the technical hydrogen capacity of methanol is higher than the hydrogen capacity of ammonia which is only 17.8 wt%.<sup>28</sup> Note, that there is no chance to produce extra hydrogen by adding water to an ammonia cracking process. This generation of additional H<sub>2</sub> from water is only possible for carriers that release hydrogen by steam reforming, what is undoubtedly the state-of-the-art process for hydrocarbons, alcohols and ethers.

Developing the idea of extra hydrogen production from water even further, DME can be regarded as a very attractive storage molecule. DME is produced from two mols of methanol by splitting off water (dehydration) at the energy-rich location. Consequently, hydrogen production from DME involves the splitting of DME with one mol of water to two mols of methanol in the first step, and subsequent steam reforming of methanol with two extra mols of added water. As shown in Fig. 1, the total sequence offers the potential to liberate two mols of CO<sub>2</sub> and six mols of H<sub>2</sub> from one mol of DME, resulting in a technical hydrogen storage capacity of DME of 26.1 wt%. Impressively, this value is 47% higher than the hydrogen storage capacity of ammonia.

#### Methanol steam reforming



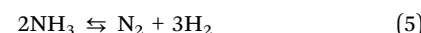
$$M_{\text{CH}_3\text{OH}} = 32 \text{ g mol}^{-1} \quad 3 \cdot M_{\text{H}_2} = 6 \text{ g mol}^{-1} \quad W_{\text{H}_2, \text{technical}} = 18.8 \text{ wt\%}$$

#### DME steam reforming



$$M_{\text{CH}_3\text{OCH}_3} = 46 \text{ g mol}^{-1} \quad 6 \cdot M_{\text{H}_2} = 12 \text{ g mol}^{-1} \quad W_{\text{H}_2, \text{technical}} = 26.1 \text{ wt\%}$$

#### Ammonia decomposition



$$M_{\text{NH}_3} = 17 \text{ g mol}^{-1} \quad 1.5 \cdot M_{\text{H}_2} = 3 \text{ g mol}^{-1} \quad W_{\text{H}_2, \text{technical}} = 17.8 \text{ wt\%}$$

Note, that hydrogen release from all the carriers is an endothermic process, why the energy required for this step at the place of energy consumption needs to be taken into account. Here it might be interesting to compare the energy required, to release hydrogen from the DME/H<sub>2</sub>O mixture to the energy demand of the water electrolysis step at the place of energy generation. The comparison of the endothermic reaction enthalpies, required to produce one mol of hydrogen by water electrolysis (+285.8 kJ mol<sub>H<sub>2</sub></sub><sup>-1</sup>) and by DME steam reforming (+20.3 kJ mol<sub>H<sub>2</sub></sub><sup>-1</sup>, see Table 2) allow a first estimation. Consequently, the release of hydrogen from water via steam reforming compared to water electrolysis is clearly more favorable in terms of energy. Therefore, energy intensive water electrolysis makes mainly sense in regions of high availability of renewable energy. The DME steam reforming step on the other hand, allows the comparably energy efficient harvesting of hydrogen from water that is locally available at the place of energy consumption.

Most available power-to-X literature to date considers DME primarily as a substitute green fuel for diesel engines.<sup>31</sup> Undoubtedly, such application is interesting to use cleaner fuels in existing diesel engines. It is a matter of fact, however, that the use of DME as diesel substitute for combustion engines leads to a highly distributed emission of CO<sub>2</sub>. Thus, DME as combustion fuel is only sustainable if the CO<sub>2</sub> has been extracted from biogenic sources or from the atmosphere. Alternative attempts to use CO<sub>2</sub> from fossil resources, e.g. captured from exhaust gas of coal fired power plants, only



add an additional use cycle to the fossil CO<sub>2</sub> emission. Since biogenic CO<sub>2</sub> sources are dependent on local conditions, often limited, and difficult to transport, CO<sub>2</sub> from the atmosphere (Direct Air Capture, DAC) will be the necessary step for such a sustainable cycle, at least for large scale applications. DAC, however, is yet expensive in both investment and operation cost and may stay expensive due to the low concentration of CO<sub>2</sub> in the atmosphere (about 420 ppm compared to *ca.* 78 vol% in the case of nitrogen for ammonia production).

In general, we can state based on a literature survey that most hydrogen storage concepts using CO<sub>2</sub> suffer from the high cost for its fully carbon-neutral isolation from the atmosphere.<sup>32–35</sup> Estimations of capture costs show a large bandwidth across scientific literature, reflecting the early stage of technology development. Depending on the utilized technology, low-carbon energy source and DAC plant size, capture costs can range from 150 € per t to 800 € per t.<sup>32–34</sup> However, projected capture costs in the years towards 2030 will decrease substantially for the two main DAC technologies, low-temperature solid sorbent (LT) and high-temperature aqueous solution (HT), through research and development, learning by doing and economies of scale. While Carbon Engineering, the major technology vendor of HT-DAC, projects future capture costs of 94–170 € per t, Climeworks, one prominent LT-DAC supplier, projects costs of around 100 € per t.<sup>33,34,36</sup> Other studies predict CO<sub>2</sub> costs of 150 to 200 € per ton by 2030.<sup>37,38</sup> Whether this significant cost reduction will become reality in utility-scale operational plants has to be evaluated after first commercial plants have been commissioned.

### State-of-the-art of DME synthesis and DME reforming

**DME synthesis.** DME is commercially produced *via* the acid catalyzed dehydration of MeOH. In the conventional indirect route, MeOH is first synthesized, purified and then dehydrated in a separate reactor. All commercial scale DME plants use this indirect route.<sup>39</sup> In the related industrial processes, water is removed from the crude MeOH by means of distillation and pure MeOH is evaporated and preheated before entering a fixed bed reactor. Here, MeOH is dehydrated in a gas-phase reaction at a temperature between 220 and 360 °C and pressures up to 20 bar.<sup>39</sup> Since the reaction is equilibrium-limited, the multi-component reaction product needs to be separated in a two-step distillation process.<sup>40</sup>

The more recently developed direct route in contrast, realizes the synthesis of DME from syngas in a single reactor. Here, MeOH synthesis, WGS reaction, and MeOH dehydration occur in parallel. The reactor can either contain a physical mixture of a MeOH synthesis catalyst and a dehydration catalyst or can operate with a bifunctional catalyst combining both functionalities.<sup>41</sup> While one reactor can be omitted in comparison to the indirect route, the purification process for the direct route is more challenging. Due to the presence of DME with its high vapor pressure, a simple flash separation of unreacted syngas is not feasible, since significant amounts of DME would be recycled to the reactor.<sup>42</sup> For conventional CO-rich syngas, the advantage of the direct route is the synergistic interplay of

the involved reactions, leading to a higher syngas conversion. For CO<sub>2</sub>-utilisation, however, the synergistic interplay of the reactions is less pronounced, since the reverse WGS dominates over the WGS. Consequently, instead of consuming the water from the dehydration reaction, additional water is generated, leading to a thermodynamic inhibition.<sup>39,43</sup>

Emerging production routes focus on the coupling of reaction and separation. Hereby, sorption-based<sup>44–46</sup> and membrane-based<sup>47,48</sup> methods have been investigated. A particular promising approach in the scope of CO<sub>2</sub>-utilisation is the DME synthesis *via* reactive distillation. Through *in situ* removal of the reaction products from the chemical equilibrium, a full MeOH conversion can be achieved. While classical DME synthesis from methanol requires one dehydration reactor and two distillation columns, reactive distillation allows the production of purified DME in a single unit operation. Furthermore, since water is removed in the reactive distillation column, water containing crude MeOH can directly be used as a feedstock, thus omitting a dedicated crude MeOH distillation column (see ESI,† Fig. S4). Besides the drastic process simplification, this entails the advantage of reducing the reboiler duty by the exothermic dehydration reaction inside the column. Furthermore, the reaction occurs in the liquid phase, thus the energy-intensive evaporation of the MeOH feedstock is not required.<sup>49</sup>

### DME steam reforming

Hydrogen release from DME is carried out *via* steam reforming. Hydrogen yields of above 99% have been demonstrated with H<sub>2</sub> concentrations at the reactor outlet of 75 vol%. Typical reaction conditions are in the range of 250–400 °C, at near ambient pressures. Most studies have applied fixed-bed reactors.<sup>30,50</sup> In DME steam reforming, the reaction propagates in two steps. The hydrolysis of DME to methanol is followed by steam reforming of methanol forming CO<sub>2</sub> and H<sub>2</sub>. Side reactions such as DME or methanol decomposition, CO<sub>x</sub> methanation or the water-gas-shift reaction can occur and depend on the applied catalyst. Over-stoichiometric steam-to-DME feed ratios are favourable to suppress side reactions and to increase hydrogen yields.<sup>30</sup>

For DME steam reforming, two catalytic functionalities are required. While the hydrolysis is catalysed by an acidic function (*e.g.* H-zeolites or γ-Al<sub>2</sub>O<sub>3</sub>), the reforming step proceeds over metallic active centres (*e.g.* Cu-, Pd-based).<sup>50</sup> Consequently, bifunctional catalyst materials or physical mixtures of two heterogeneous catalysts are used. For DME hydrolysis, acidic zeolites are more active than γ-Al<sub>2</sub>O<sub>3</sub>, but prone to coking and hydrocarbon formation.<sup>50</sup> For γ-Al<sub>2</sub>O<sub>3</sub>, however, higher temperatures (about 350 °C) are required to reach sufficient activity. For the reforming step Cu/ZnO/Al<sub>2</sub>O<sub>3</sub> and spinel-type catalysts are discussed in the literature but deactivation by sintering, coking or changes in oxidation state of the active metal leave much room for further catalyst development.<sup>51–53</sup> Besides copper, noble metals like palladium<sup>54,55</sup> or platinum<sup>56,57</sup> have been applied in DME steam reforming as well. In general, the development of stable and highly active



**Table 1** Physico-chemical properties of liquefied DME and CO<sub>2</sub>. BOG: boil-off gas, GWP<sub>100</sub>: global warming potential, LHV: lower heating value, T<sub>BP</sub>: boiling temperature

Component	T <sub>BP</sub> /°C	Liquid density/kg m <sup>-3</sup>	Viscosity at T <sub>BP</sub> /mPa s	LHV/MJ kg <sup>-1</sup>	GWP <sub>100</sub> /CO <sub>2</sub> -equiv.	Transportation BOG/% d <sup>-1</sup>
CO <sub>2</sub>	−55 to −50 <sup>a</sup>	1178	0.24	—	1.0	0.12 <sup>58–59</sup>
DME	−24	735	0.19	28.9	0.3	0.017 <sup>60</sup>
MeOH	64	805	0.52 <sup>b</sup>	19.9	2.97	0.0005 <sup>60</sup>
NH <sub>3</sub>	−34	683	0.26	18.6	0	0.025 <sup>60</sup>

<sup>a</sup> At 7–8 bar. <sup>b</sup> At 25 °C.

DME steam reforming catalyst materials is a matter of current intense R&D activities.

### Closed CO<sub>2</sub> cycle as competitive advantage

In this contribution, we propose DME as a transport vector for a large-scale and long-distance point-to-point hydrogen transport. In this scenario, the excellent technical hydrogen storage capacity of DME is used to ship hydrogen from an export harbour to an import harbour, where DME steam reforming takes place. The herein obtained gas mixture contains mainly CO<sub>2</sub> and H<sub>2</sub>. Purification of the released hydrogen to pipeline quality will also provide pure CO<sub>2</sub> (Fig. 1). Instead of releasing the CO<sub>2</sub> into the atmosphere, we propose its liquefaction and refilling into the same ship. After back-shipping, this CO<sub>2</sub> should be used for another round of hydrogen transport. With this closed CO<sub>2</sub> cycle concept, DAC at the export harbour is only necessary to refill CO<sub>2</sub> losses. The greatest part of the required CO<sub>2</sub> for the next shipping cycle is provided by recycled and back-shipped CO<sub>2</sub>. Note, that the CO<sub>2</sub> back shipping creates no extra transport needs if the same ship can be applied for DME and CO<sub>2</sub> shipping, as the transport ship must return anyway. A particularly attractive feature of the here proposed DME/CO<sub>2</sub> hydrogen storage and transport cycle is, that the physico-chemical properties of liquefied DME and liquefied CO<sub>2</sub> are similar. Some properties that are important with regard to shipping handling of hydrogen carriers at harbours are shown in Table 1. To emphasise the attractiveness of the proposed DME/CO<sub>2</sub> storage cycle, a comparison with the known hydrogen carriers MeOH and ammonia is also given.

Commercially operating CO<sub>2</sub> tankers so far transport relatively small quantities of food grade liquid CO<sub>2</sub> at medium pressure (15–20 bar and −30 °C).<sup>61</sup> However, this medium pressure range is considered impractical for ship sizes above 10.000 t CO<sub>2</sub>.<sup>62</sup> For large scale CO<sub>2</sub> shipping, the literature suggests to use even lower temperatures and pressures around 6 to 8 bar and −55 to −50 °C.<sup>61,63</sup> At such low temperatures, it is key to avoid the formation of solid CO<sub>2</sub> (as dry ice or hydrates) to prevent blockages.<sup>64</sup> First vessels specialized for application under such conditions are currently under construction, *e.g.* by Mitsubishi Heavy Industries, Kawasaki Kisen Kaisha and Equinor.<sup>65–67</sup> In addition, the International Organisation for Standardization has convened a working group (ISO/TC 265/WG 7) on the transport of CO<sub>2</sub> by ship in order to better understand the technical requirements for a future CO<sub>2</sub> shipping standard.<sup>68</sup>

As Table 1 shows, DME can be liquefied under ambient pressure at a temperature of −25 °C. The viscosity of liquid

DME (0.19 mPa s) is very similar to liquid CO<sub>2</sub> (0.24 mPa s), potentially allowing the use of the same pumping equipment for DME and CO<sub>2</sub> at the port facilities. A larger difference is to be noticed in the liquid densities of both substances ( $\rho_{\text{CO}_2} = 1178 \text{ kg m}^{-3}$  and  $\rho_{\text{DME}} = 735 \text{ kg m}^{-3}$ ). Volatileness is addressed by giving the boil-off gas (BOG), comparing the carrier losses during transportation *via* shipping. Although the tanks are insulated, a small amount of warming occurs, causing the carrier to evaporate as it reaches its boiling point. This natural evaporation, known as boil-off, is unavoidable, and the generated BOG must be removed to preserve the tanks' pressure. The BOG value is mainly a function of the boiling point of the components. Literature suggests boil-off losses of 0.017% per day for the DME transport<sup>60</sup> while CO<sub>2</sub> losses are slightly higher with 0.12–0.15% per day.<sup>58,59</sup> To evaluate the harm of BOG and potential further losses during the transport and storage cycle on the climate, we have additionally given the global warming potential of the vectors. Here, DME shows a moderate value of 0.3 CO<sub>2</sub>-equiv.

Typical type C pressure vessels that can be used on ships are made of some aluminium alloy, stainless steel or nickel-steel. With regard to corrodibility, DME and CO<sub>2</sub>, but also NH<sub>3</sub> are both compatible at least with stainless steel and aluminium.<sup>70</sup> Shipping and handling of DME and CO<sub>2</sub> alone is well established and there are no material compatibility issues.

The handling and shipping of DME is reported to be very similar to LPG.<sup>42</sup> However, modification of the existing LPG infrastructure may be necessary for DME handling. For example, nitrile rubber (NBR) and fluoro rubber (FKM) sealings are used in some LPG facilities today, but are known to swell in contact with DME.<sup>69</sup> In contrast, polytetrafluoroethylene (PTFE), polychlorotri-fluoroethylene (PCTFE) and polyvinylidene fluoride (PVDF) were found to provide satisfactory stability in combination with both, DME and CO<sub>2</sub>.<sup>69,70</sup> Consequently, the reuse of existing LPG ships to meet the requirements for carrying both, DME and CO<sub>2</sub> may be technically feasible,<sup>71</sup> and a solution, which is quickly implementable. Alternatively, the construction of new multi gas carrier ships that are fully optimized for the transport of these substances appears attractive. This high degree of compatibility makes the future utilisation of the same shipping and port facilities for liquefied DME and CO<sub>2</sub> realistic.

### Water management aspects using DME as hydrogen vector

In the considered scenario of large-scale hydrogen generation from renewables, high amounts of fresh water are required for electrolysis. According to the literature, about one kg of water is



needed per standard cubic meter of hydrogen gas ( $0.0899 \text{ kg H}_2$ ).<sup>72</sup> It is a matter of fact that many global areas that are rich in renewable power from wind and sun are scarce in fresh water. Close to sea harbour ports electrolysis may be always operable using sea water after desalination.<sup>73</sup> Furthermore, large amounts of brine are produced as by-product of desalination, which comes with adverse impact on the local environment and/or with high capital cost for brine disposal.<sup>74</sup> Therefore, hydrogen production and shipping strategies that reduce the local demand of desalinated water are highly desired.

In this context, the use of the DME/ $\text{CO}_2$  hydrogen storage cycle offers a very attractive way to reduce the required amount of fresh water at the hydrogen production site. As shown in Fig. 1, the production of one mol of DME requires six mols of water to provide the necessary amount of hydrogen. At the same time, the energy-dense ‘packing’ of hydrogen in the form of DME releases 3 mols of water as a by-product of the synthesis. This water can be recycled for further use in the electrolysis. Thus, compared to  $\text{H}_2$  shipping, *e.g.* in the form of ammonia or cryogenic hydrogen, only half of the water is needed at the production site to make a given mass of hydrogen available at the place of energy consumption. Note, that the here-proposed concept requires addition of water at the destination of the hydrogen transport, where DME reforming takes place to meet a given hydrogen demand. For most future hydrogen transport scenarios, this is not considered a major problem, as many energy-hungry hydrogen destinations are comparatively rich in freshwater (*e.g.* Europe, Japan, China's East Coast, US West Coast).

A further relevant consideration for water provision in the here proposed concept arises from the  $\text{CO}_2$  loss compensation by DAC, according to Fig. 1. Loss compensation might be necessary to provide a fully sustainable hydrogen transportation cycle, *e.g.* if DME is also used for ship propulsion or if some  $\text{CO}_2$  losses occur in the various separation or transport steps of the storage cycle. Even though these quantities will be relatively small, due to the fact that most of the  $\text{CO}_2$  is kept in a closed cycle, it should be pointed out that the DAC process also captures water from the atmosphere. Filtering  $\text{CO}_2$  from the air using low temperature DAC systems is usually accompanied by

water as a side product.<sup>35</sup> This captured fresh water can be made available to the electrolysis step, reducing its net water demand. Contrarily to the almost constant global  $\text{CO}_2$  composition in air, its water content is a strong function of the air humidity and ambient conditions.

## Comparison of DME with other hydrogen vectors

Several hydrogen-rich molecules, such as ammonia, methane, methanol or Liquid Organic Hydrogen Carrier (LOHC) compounds are discussed and compared for hydrogen storage and transport today.<sup>75,76</sup> An overriding conclusion is that the results of these studies highly depend on the scenario and applications considered and on the specific assumptions made. In this paper, we will restrict our head-to-head comparison to DME, methanol and ammonia to compare hydrogen storage compounds that have existing markets as chemicals or fuels today, apart from their future potential role in hydrogen transport. A selection of important characteristic properties of these three hydrogen storage compounds, with focus on transport, hydrogen release and safety is presented in Table 2. In addition, Table S1 in the ESI† provides an overview about conditions and product composition of the carrier synthesis.

Among these three hydrogen storage compounds, DME has the lowest toxicity, the highest technical hydrogen capacity (see eqn (3)–(5)) and the second lowest heat requirement for hydrogen release. The temperature level for hydrogen release from DME is in a similar range as for hydrogen release from methanol, but significantly milder compared to ammonia. A comparison of energy content per ship loading for DME, ammonia and methanol is found in Fig. S1d in the ESI.†

## Preliminary techno-economic evaluation of the DME/ $\text{CO}_2$ hydrogen storage cycle

### Methodology

The objective of this evaluation is to identify the specific energy and material consumption to deliver a ton of  $\text{H}_2$  at the

**Table 2** Characteristic properties of hydrogen storage using ammonia, methanol or DME

Hydrogen carrier [aggregation state at 20 °C]	Mols of released $\text{H}_2$ per mol of carrier <sup>a</sup>	Gravimetric energy density <sup>a</sup> ( $\text{kW h kg}^{-1}$ )	Heat required for $\text{H}_2$ release ( $\text{kJ mol}^{-1} \text{H}_2^{-1}$ )	Liquid density at 20 °C ( $\text{kg L}^{-1}$ )	Volumetric energy density <sup>a</sup> ( $\text{kW h L}^{-1}$ )	Temperature of $\text{H}_2$ release	Safety aspects
Ammonia [liquefied]	1.5	5.9	30.8	0.68	4.0	400–600 °C <sup>77</sup>	
Methanol [liquid]	3	6.2	16.3	0.79	4.9	250–300 °C	
Dimethyl ether (DME) [liquefied]	6	8.7	20.3	0.73	6.3	250–400 °C	

<sup>a</sup> Including hydrogen formation from water in the reforming step.



utilisation point starting from the primary raw materials and renewable energy at the point of generation. Along the evaluation, the following system boundaries are considered: renewable electricity provides the power demand for all subprocesses, including seawater desalination; H<sub>2</sub> production via H<sub>2</sub>O electrolysis; capture of CO<sub>2</sub> from ambient air; production of DME from H<sub>2</sub> and CO<sub>2</sub>; shipping of DME to the utilisation point, and DME reforming at the utilisation point. The CO<sub>2</sub> for DME synthesis is mainly provided by back-shipping. For this study, cumulative CO<sub>2</sub> losses during DME reforming and DME/CO<sub>2</sub> shipping of 3% are assumed. DAC provides the make-up CO<sub>2</sub>-stream to compensate for these losses. Also 3% of the produced H<sub>2</sub> are assumed as losses during reforming on the utilisation site, reflecting purging effects and separation efficiency.

The specific heat and electricity demands of DME and MeOH synthesis are taken from literature.<sup>78</sup> For NH<sub>3</sub>, the demand is based on own process simulation of a conventional Haber–Bosch loop supported by an air separation unit (ASU) using Aspen Plus® as described in ESI.† The shipping specific energy demand for each H<sub>2</sub> carrier considered is evaluated based on the net diesel consumption for the transport distance of one way and the tankers capacities considered in Table 4. The specific energy demand for the reforming process of the considered components is evaluated based on our own simulation using Aspen Plus® and according to literature conditions as given in Table 2 and in the ESI,† Table S2. The energy demand of the separation of H<sub>2</sub> and CO<sub>2</sub>/N<sub>2</sub> after the reforming step is not considered in this evaluation. The CO<sub>2</sub> liquefaction specific energy demand in the case of DME/CO<sub>2</sub> cycle was evaluated using Aspen®.

The energy efficiency of the considered value chain for DME, methanol and ammonia is calculated using eqn (6):

$$\eta_{\text{energy}} = \frac{\sum_i m_{H_2} \cdot LHV_{H_2}}{\sum_j Q_j + \sum_k W_k + \sum_l m_l \cdot LHV_l} \quad (6)$$

where  $m$  denotes the mass flow rate of the primary feedstock  $l$  and the H<sub>2</sub> delivered at the utilisation point. LHV is the lower heating value at 298 K, while  $Q$  and  $W$  represent externally supplied heat fluxes and electric power demand along the value chain accounting for energy demand for water desalination, electrolysis, synthesis process, transport specific energy demand, reforming demand, and the liquefaction energy demand as in case of a DME/CO<sub>2</sub> closed cycle. This efficiency reflects the amount of energy utilized along the value chain relative to the chemical energy content of the H<sub>2</sub> arrived at the utilisation point. The key assumptions for the material and energy evaluation are listed in the ESI,† Table S4.

Furthermore, the cost of production of the respective H<sub>2</sub> carriers are evaluated as a function of feedstock cost based on a stoichiometric analysis. The shipping cost are evaluated based on specific tanker capacity, capital investments, fuel consumption and other factors as elaborated in Table S3 of the ESI† and described in our previous publications.<sup>79,80</sup> The production cost was evaluated against variable cost of feedstock to reflect

several other aspects, such as the cost of renewable power, capital investments, capacity factors, geographical related financial aspects and other significant factors. This simplification gives a linear function presented in eqn (7):

$$C_{tx} = \alpha_{H_2} \times C_{H_2} + \beta_{CO_2} \times C_{CO_2} + \gamma_{N_2} \times C_{N_2} + C_{transp_x} \quad (7)$$

where  $C_{tx}$  represents the production cost of X product in € per ton.  $\alpha_{H_2}$ ,  $\beta_{CO_2}$  and  $\gamma_{N_2}$  represents the stoichiometric factor for H<sub>2</sub>, CO<sub>2</sub> and N<sub>2</sub> in the net reaction to produce X according to eqn (3)–(5).  $C_{H_2}$ ,  $C_{CO_2}$  and  $C_{N_2}$  represents the feedstock cost of H<sub>2</sub>, CO<sub>2</sub> and N<sub>2</sub> in € per ton, respectively. The  $C_{transp_x}$  represents the specific cost of transport in € per ton for a certain product X and for a distance of 20 000 km in this specific evaluation.

## Results

Table 3 summarises the material and energy balance for MeOH, NH<sub>3</sub> and DME per ton of H<sub>2</sub> released at the point of utilisation.

The DME/CO<sub>2</sub> cycle profits from its high energy density, the water side production and the closed CO<sub>2</sub> cycle. At the point of hydrogen production, the demand for water desalination is almost 27% lower for DME than for MeOH production and 82% lower than for NH<sub>3</sub> production, based on the same amount of H<sub>2</sub> delivery. The net H<sub>2</sub>O demand at the export harbour is different between the considered vectors due to the stoichiometric formation of water in the case of MeOH and DME according to eqn (3)–(5). This water can be recycled for the electrolysis step, lowering the desalination effort. The net H<sub>2</sub>O demand from desalination is the lowest in case of DME.

A further aspect is, that around 97% less CO<sub>2</sub> is required at the point of generation compared to the here-considered MeOH case without CO<sub>2</sub> back-shipping. One may argue that CO<sub>2</sub> back-shipping can also be considered after MeOH reforming. However, the quite different physico-chemical properties of MeOH and CO<sub>2</sub> suggest that a common methanol tanker is not suitable for CO<sub>2</sub> back shipping. Thus, in the worst case, the back-shipping in case of MeOH would require an additional tanker with empty returns of both ships. Importantly, the net energy delivered at the utilisation point is the highest in case of DME. For each ton of H<sub>2</sub> delivered using DME as a carrier, around 55% of this energy arrives at the point of utilisation after considering all the consuming sub-processes along the value chain. The cases of MeOH and NH<sub>3</sub> only reach energy efficiencies of 46% and 50%, respectively.

For the economic evaluation, the cost of delivery for 1 ton of H<sub>2</sub> released at the utilisation point was calculated for DME, MeOH and NH<sub>3</sub>. Assuming the same losses of H<sub>2</sub> for the three vectors, 1.03 tons of H<sub>2</sub> are needed to be produced at the point of production. The required net amounts of CO<sub>2</sub> or N<sub>2</sub> is taken from the material balance evaluation in Table 3. In Fig. 2, the H<sub>2</sub> costs are varied for calculating the cost of hydrogen delivery for all three hydrogen carriers. The calculations use the current DAC-based CO<sub>2</sub> cost of 720 € per ton and at the N<sub>2</sub> cost from ASU at 200 € per ton (as adopted from Mantei *et al.*<sup>79</sup>



**Table 3** Material and energy balance overview comparing MeOH, NH<sub>3</sub> and DME (X) per ton of released hydrogen at the point of utilisation

H <sub>2</sub> carrier	MeOH	NH <sub>3</sub>	DME
<b>Material balance</b>			
H <sub>2</sub> release at utilisation point [t]	1	1	1
X demand [t t <sup>-1</sup> H <sub>2</sub> rel.]	5.51	5.85	3.95
Net H <sub>2</sub> O demand <sup>a</sup> [t H <sub>2</sub> O t <sup>-1</sup> H <sub>2</sub> rel.]	7.20	10.30	5.67
Net CO <sub>2</sub> demand [t CO <sub>2</sub> t <sup>-1</sup> H <sub>2</sub> rel.]	7.57	—	0.22 <sup>b</sup>
N <sub>2</sub> demand [t N <sub>2</sub> t <sup>-1</sup> H <sub>2</sub> rel.]	—	4.82	—
O <sub>2</sub> side product [t O <sub>2</sub> t <sup>-1</sup> H <sub>2</sub> rel.]	8.24	8.24	8.24
<b>Energy balance</b>			
Water desalination [MW h <sub>el</sub> m <sup>-3</sup> H <sub>2</sub> O] at place of energy generation	0.36	0.52	0.28
Specific electrolyzer demand at place of energy generation [MW h t <sup>-1</sup> H <sub>2</sub> ]	51.5	51.5	51.5
<b>DAC</b>			
[MW h <sub>el</sub> t <sup>-1</sup> CO <sub>2,DAC</sub> , for 1 t H <sub>2</sub> rel.]	3.786	—	0.113
[MW h <sub>th</sub> t <sup>-1</sup> CO <sub>2,DAC</sub> for 1 t H <sub>2</sub> rel.]	11.360	—	0.340
<b>Synthesis process at place of energy generation</b>			
[MW h <sub>el</sub> t <sup>-1</sup> H <sub>2</sub> rel.]	0.851	4.671 <sup>d</sup>	0.854
[MW h <sub>th</sub> t <sup>-1</sup> H <sub>2</sub> rel.]	-2.674	3.319 <sup>d</sup>	-1.138
<b>Shipping</b>			
[MW h <sub>total</sub> t <sup>-1</sup> H <sub>2</sub> rel.] <sup>c</sup>	0.824	1.791	1.128
<b>Reforming/cracking process at place of energy demand</b>			
[MW h <sub>total</sub> t <sup>-1</sup> H <sub>2</sub> rel.]	6.283	5.178	6.356
<b>Liquefaction of CO<sub>2</sub> at place of energy demand</b>			
[MW h <sub>total</sub> t <sup>-1</sup> H <sub>2</sub> rel.]	—	—	1.679
Energy efficiency [%], eqn (6)	46.09	49.75	54.52

<sup>a</sup> Net water demand at the export harbor. <sup>b</sup> Closed CO<sub>2</sub> cycle considering 3% CO<sub>2</sub> losses. <sup>c</sup> Based on specific diesel consumption for one way and considering different tanker capacities for X transport. <sup>d</sup> Including air separation unit demand.

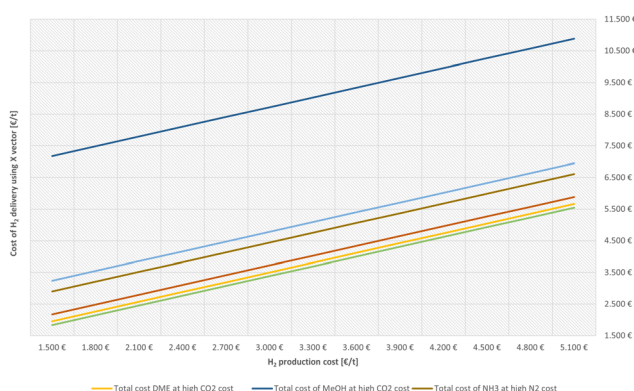


**Fig. 2** Cost of delivery of 1 ton of H<sub>2</sub> at the point of utilisation as a function of H<sub>2</sub> production cost considering the different carriers DME, MeOH and NH<sub>3</sub>. Low CO<sub>2</sub> DAC cost assumed 200 € per t, high CO<sub>2</sub> DAC cost at 720 € per t. Low N<sub>2</sub> cost assumed 50 € per t, high N<sub>2</sub> cost at 200 € per t.

and Ouda *et al.*<sup>81</sup>). Note, that some predictions for the future development of DAC technologies calculate CO<sub>2</sub> cost of 150 to 200 € per ton by 2030.<sup>37,38</sup> A sensitivity study covering the low and high feedstock CO<sub>2</sub> and N<sub>2</sub> cost influence on the cost of H<sub>2</sub> delivery using vector X is provided in Fig. S3d in the ESI†. The results displayed in Fig. 2 and in Fig. S3d (ESI†) reflect the benefits of the closed CO<sub>2</sub> cycle considered in the case of DME as H<sub>2</sub> carrier. The specific transport cost in € per t of DME over

20 000 km to deliver 1 ton of H<sub>2</sub> at the utilization point is around 36% less than that of NH<sub>3</sub> at the same tanker capacity.

The shipping cost evaluation methodology is given in Table S3 in the ESI† and was introduced by Hank *et al.*<sup>80</sup> The simplified eqn (7) was applied to evaluate the total cost for the delivery of a ton of H<sub>2</sub> at the utilisation point. This is directly correlated to the higher energy density of DME.

For the closed DME/CO<sub>2</sub> transport cycle, Fig. 3 illustrates the contribution of different cost shares, namely H<sub>2</sub> production, CO<sub>2</sub> provision and shipping, to the total cost as a function of

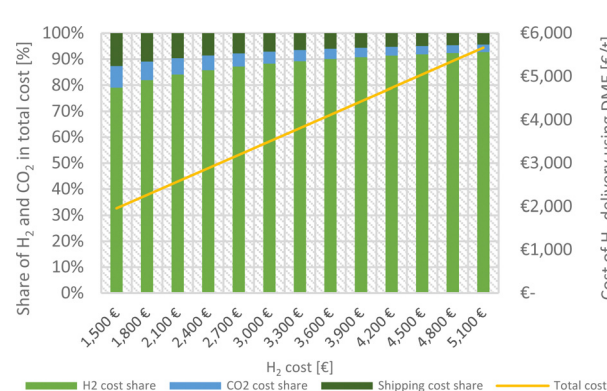


**Fig. 3** The cost structure for delivery of 1 ton of H<sub>2</sub> at the utilisation point using DME as H<sub>2</sub> carrier in a closed DME/CO<sub>2</sub> cycle as a function of H<sub>2</sub> cost and CO<sub>2</sub> costs by DAC high at 720 € per t<sub>CO<sub>2</sub></sub>.



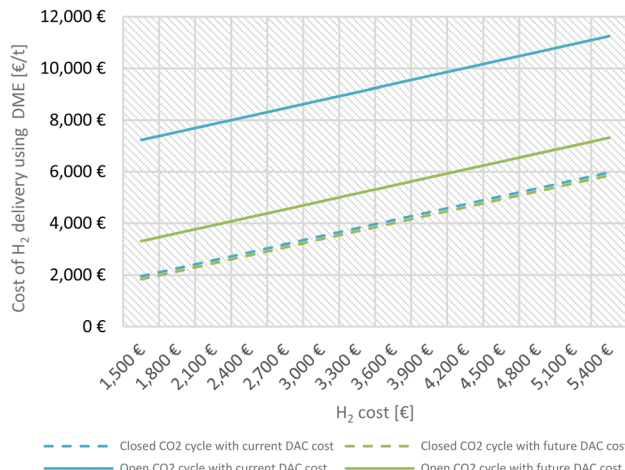


Fig. 4 The cost structure for delivery of 1 ton of H<sub>2</sub> at the utilisation point using DME as H<sub>2</sub> carrier as a function of H<sub>2</sub> cost. Two DAC cost values, 720 € per t (current) and 200 € per t (future), and CO<sub>2</sub> losses in the cycle of 3% are assumed. Comparison of the scenarios including full CO<sub>2</sub> back-shipping (closed) and CO<sub>2</sub> recovery exclusively from DAC (open).

the hydrogen delivery cost. While H<sub>2</sub> production naturally comprises the highest cost share, shipping and CO<sub>2</sub> provision account in summary for above 20%, if the H<sub>2</sub> production cost is low (here 1500 €).

The low share of cost for CO<sub>2</sub> provision is also a result of the described closed transport cycle, including CO<sub>2</sub> back-shipping. To highlight the significant influence of the closed DME/CO<sub>2</sub> cycle in our concept, Fig. 4 shows the cost of H<sub>2</sub> delivery for a closed cycle (including CO<sub>2</sub> back-shipping) and an open cycle (using CO<sub>2</sub> exclusively from DAC). For DAC cost two values were assumed: 720 € per t<sub>CO<sub>2</sub></sub>, reflecting a current price and 200 € per t<sub>CO<sub>2</sub></sub>, reflecting an optimistic future price for DAC.<sup>79,81</sup>

Considering todays DAC cost, the CO<sub>2</sub> back-shipping has the potential to reduce the H<sub>2</sub> delivery cost by up to 56%. Assuming a cost reduction for DAC processes to 200 € per t<sub>CO<sub>2</sub></sub> within the next decade, a price reduction of up to 26% by the CO<sub>2</sub> back-transportation is achieved.

The variation of CO<sub>2</sub> cost against H<sub>2</sub> delivery cost for DME as a carrier was also evaluated at constant H<sub>2</sub> production cost, further illustrating the positive effect of the closed cycle. These calculations are shown in Fig. S2c in the ESI.<sup>†</sup> Since only make-up CO<sub>2</sub> is produced by DAC in the here considered DME case including CO<sub>2</sub> back-shipping, the influence of CO<sub>2</sub> cost variation is not significant and reaches about 5% of the production cost at the current considered CO<sub>2</sub> cost of 720 € per ton (Fig. S2c in ESI<sup>†</sup>).

In general, our evaluation shows that under stoichiometric conditions, H<sub>2</sub> delivery cost over 20 000 km can be very attractive using the here proposed DME/CO<sub>2</sub> cycle even under the currently high cost of CO<sub>2</sub> based on DAC. At global sweet spots with H<sub>2</sub> production costs below 3000 € per ton, delivery costs of H<sub>2</sub> at the point of utilisation under 3500 € per ton are achievable. Variation of shipping distance to 10 000 km does not have a significant influence on the total cost since the share of shipping cost is ranging between 1.5–12% of the net production cost (see also Fig. S3 in the ESI<sup>†</sup>).

### Case study Australia – Europe

In the following case study, we consider the delivery of 108 ktpa of H<sub>2</sub> to Europe from Australia (transport distance of 20 000 km) by relying on typical tanker capacities for the three considered H<sub>2</sub> carriers, as shown in Table 4. Extended information about shipping cost and consumption evaluation are included in Table S3 of the ESI.<sup>†</sup>

Table 4 Case study parameters and results for the Australia – Europe H<sub>2</sub> import case

H <sub>2</sub> carrier	MeOH	NH <sub>3</sub>	DME
Shipping <sup>80</sup>			
Volume, [m <sup>3</sup> ]	140 000	84 000	84 000
Capacity X, [kt]	110.6	57.2	61.32
Transport distance, [km]	20 000	20 000	20 000
Travel time – one-way, [d]	26	26	26
Number of trips to deliver H <sub>2</sub> required per year	5	11	7
Cost of transport, [€ per t X]	32.24	66.71	62.60
Simple material and energy balance			
H <sub>2</sub> delivered at Rotterdam [ktpa]	108	108	108
X transport to Rotterdam [ktpa]	578.3	614.4	427.3
H <sub>2</sub> capacity per trip [kt per trip]	20.7	10.1	16.0
Annual losses due to boil-off [ktpa]	0.1	4.0	1.9
Energy delivered in Rotterdam [GW h a <sup>-1</sup> ]	3602.1	3583.1	3688.7
By-product O <sub>2</sub> produced by electrolysis in Australia [ktpa]	891	891	891
CO <sub>2</sub> back shipped to Australia [ktpa]	—	—	793
CO <sub>2</sub> back shipped to Australia [10 <sup>3</sup> m <sup>3</sup> a <sup>-1</sup> ]	—	—	699
Simple system layout			
Renewable generators, [MW] assuming factor 1.3 to electrolyzer capacity	1292.8	1292.8	1292.8
Electrolyzer capacity in Australia, [MW] at full load hours of 5600 h a <sup>-1</sup>	994.5	994.5	994.5
Water desalination plant capacity in Australia, [10 <sup>3</sup> × m <sup>3</sup> a <sup>-1</sup> ]	788.5	1113.8	612.1
DAC plant capacity in Australia [ktpa]	795.0	—	24.5
ASU plant capacity in Australia [ktpa]	—	505.7	—



Around 1 GW of electrolyzer capacity would be needed to produce the 108 ktpa of H<sub>2</sub> in Australia assuming annual combined renewable energy generators full load hours of 5600 h. The renewable generators combined capacity was evaluated assuming a factor 1.3 to electrolyzer capacity in-line with the evaluations given in ref. 82. Due to the side production of water by DME and MeOH at the synthesis sites in Australia, the net water demand at these places is the lowest in case of DME to deliver the same amount of H<sub>2</sub> in Rotterdam. The DAC plant to provide the make-up CO<sub>2</sub> for DME synthesis in Australia is around 32 times smaller than needed in case of methanol due to the closed CO<sub>2</sub> cycle benefit of DME. NH<sub>3</sub> production is carbon free, and no DAC plant is needed, nevertheless, a large 505 ktpa ASU plant is considered to provide the N<sub>2</sub> needed for the delivery of 108 ktpa of H<sub>2</sub> in Rotterdam *via* NH<sub>3</sub>.

## Conclusion and outlook

In this contribution, the DME/CO<sub>2</sub> hydrogen storage cycle is proposed for long distance point-to-point transport of renewable hydrogen. Renewable hydrogen is bond to CO<sub>2</sub> under formation of DME and water at a harbour site of an energy rich location. Liquefied DME shows excellent transport properties and can be shipped using available tanker and port technologies. At the destination harbour, DME steam reforming releases H<sub>2</sub> and CO<sub>2</sub>. After separation, H<sub>2</sub> is distributed *via* a domestic pipeline infrastructure while the CO<sub>2</sub> is liquefied and back-shipped to the energy-rich location. By including CO<sub>2</sub> back-shipping, the yet cost intensive DAC is only required for the make-up of CO<sub>2</sub> losses within the transport cycle. The back-shipping of CO<sub>2</sub> is facilitated by the similar physico-chemical properties of DME and CO<sub>2</sub> and significantly increases the economic competitiveness of this hydrogen logistics technology. Water management has been identified as a further advantage of the DME/CO<sub>2</sub> cycle. Applying DME as hydrogen carrier allows to reduce the demand of cost intensive and ecologically harmful sea water desalination at the place of hydrogen generation.

A head-to-head comparison with ammonia and methanol, two of the currently most discussed hydrogen carrier molecules, DME shows a higher technical hydrogen capacity, higher gravimetric energy density and lower toxicity. The high energetic efficiency as well as the comparatively low heat demand and temperature level for H<sub>2</sub> release add more advantages of the here proposed DME/CO<sub>2</sub> cycle.

Climate change requests an urgent transition to cleaner energy technologies and it is crucial to establish technologies for generation, transport and storage of renewable energy quickly. Against this requirement it is of great advantage, that many elements of the here proposed transport cycle already show high technological readiness level and good compatibility with existing infrastructures: (1) DME synthesis from CO<sub>2</sub> and H<sub>2</sub> is already under testing up to pilot demonstration scale.<sup>83</sup> (2) DME is a well-known industrial chemical with established handling procedures and known ecotoxicological properties.<sup>84</sup> (3) With regard to shipping, the LPG-like properties of DME

facilitate its large-scale use for energy logistic purposes. (4) Separation of H<sub>2</sub>/CO<sub>2</sub> gas mixtures from DME steam reforming can be performed by state-of-the-art CO<sub>2</sub>-absorption technologies, *e.g.* washing with aqueous amine solutions.<sup>85</sup>

The large-scale application of the here-proposed DME/CO<sub>2</sub> cycle requires still a significant amount of targeted research and development. The following aspects appear of particular importance: (1) intensification of the DME synthesis processes offers significant potential for cost savings. In particular, the two step DME process with reactive distillation for DME production from MeOH offers high energy and cost saving potentials. Long-term catalyst stability investigations under reactive distillation conditions are still needed. (2) For large-scale handling and transport of liquid DME and liquid CO<sub>2</sub> in port and ship infrastructures, material compatibility questions have to be addressed in more detail. An important development goal is to adapt existing infrastructures from fossil LPG applications to the new storage cycle at lowest cost and highest operational safety. (3) Further developments of active, selective and stable DME steam reforming catalysts are needed; in particular, catalyst operation at close to stoichiometric H<sub>2</sub>O/DME feed ratios is desired to reduce the energy demand for steam generation and heating. (4) Clever reactor and process design will save equipment and auxiliary energy cost; heat integration options with high temperature industrial production processes should be evaluated. (5) The effects of technical feedstock quality, side product formation or transport cross-contamination issues on process stability has to be investigated. (6) More detailed techno-economic assessments that are based on real-life mass and heat flows (including detailed heat networks, separation steps as well as auxiliary process equipment) are needed.

To gain these insights, it is necessary to investigate the DME/CO<sub>2</sub> cycle in pilot plants on relevant scale and over relevant periods of time. This admittedly large effort is justified, in our views, by the highly interesting potential of this innovative hydrogen storage and transport technology. If successfully developed and implemented, the technology will open cheaper and more efficient hydrogen transportation pathways to facilitate the global energy transition.

## Author contributions

Conceptualization: PS, RS, MS, AS, RS, ST, MA, CH, PW, OS.

Methodology: PS, RS, MS, AS, RS, ST, MA, CH, PW, OS. Project administration: PS, CH, PW, OS. Supervision: PS, CH, PW, OS.

Writing – original draft: PS, AS, ST, MA, CH, PW, OS.

## Conflicts of interest

There are no conflicts to declare.

## Note added after first publication

This article replaces the version published on 9th June 2023, which contained errors in the x-axis of Fig. 2.



## Notes and references

- 1 S. Atilhan, S. Park, M. M. El-Halwagi, M. Atilhan, M. Moore and R. B. Nielsen, *Curr. Opin. Chem. Eng.*, 2021, **31**, 100668.
- 2 M. van der Spek, C. Banet, C. Bauer, P. Gabrielli, W. Goldthorpe, M. Mazzotti, S. T. Munkejord, N. A. Røkke, N. Shah, N. Sunny, D. Sutter, J. M. Trusler and M. Gazzani, *Energy Environ. Sci.*, 2022, **15**, 1034–1077.
- 3 S. Öberg, M. Odenberger and F. Johnsson, *Int. J. Hydrogen Energy*, 2022, **47**, 624–644.
- 4 J. Hoelzen, D. Silberhorn, T. Zill, B. Bensmann and R. Hanke-Rauschenbach, *Int. J. Hydrogen Energy*, 2022, **47**, 3108–3130.
- 5 F. Swennenhuis, V. de Gooyert and H. de Coninck, *Energy Res. Social Sci.*, 2022, **88**, 102598.
- 6 A. Bhaskar, M. Assadi and H. Nikpey Somehsaraei, *Energies*, 2020, **13**, 758.
- 7 International Energy agency, Global Hydrogen Review 2022, 2022, <https://www.iea.org/events/global-hydrogen-review-2022>, (accessed 27.3.2023).
- 8 S. D. Angeli, G. Monteleone, A. Giaconia and A. A. Lemonidou, *Int. J. Hydrogen Energy*, 2014, **39**, 1979–1997.
- 9 B. C. Tashie-Lewis and S. G. Nnabuife, *Chem. Eng. J. Adv.*, 2021, **8**, 100172.
- 10 International Energy agency, Global Energy Review: CO2 Emissions in 2021, 2021, <https://www.iea.org/news/global-co2-emissions-rebounded-to-their-highest-level-in-history-in-2021> (accessed 27.3.2023).
- 11 R. Soltani, M. A. Rosen and I. Dincer, *Int. J. Hydrogen Energy*, 2014, **39**, 20266–20275.
- 12 Z. Navas-Anguita, D. García-Gusano, J. Dufour and D. Iribarren, *Sci. Total Environ.*, 2021, **771**, 145432.
- 13 G. U. Ingale, H.-M. Kwon, S. Jeong, D. Park, W. Kim, B. Bang, Y.-I. Lim, S. W. Kim, Y.-B. Kang, J. Mun, S. Jun and U. Lee, *Energies*, 2022, **15**, 8679.
- 14 M. Yu, K. Wang and H. Vredenburg, *Int. J. Hydrogen Energy*, 2021, **46**, 21261–21273.
- 15 G. Kakoulaki, I. Kougias, N. Taylor, F. Dolci, J. Moya and A. Jäger-Waldau, *Energy Convers. Manage.*, 2021, **228**, 113649.
- 16 R. Bhandari, *Renewable Energy*, 2022, **196**, 800–811.
- 17 European Parliament, Renewable Energy Directive, P9\_TA(2022)0317, 2022.
- 18 A. Tremel, P. Wasserscheid, M. Baldauf and T. Hammer, *Int. J. Hydrogen Energy*, 2015, **40**, 11457–11464.
- 19 A. Sternberg, C. M. Jens and A. Bardow, *Green Chem.*, 2017, **19**, 2244–2259.
- 20 V. L. Meca, R. d'Amore-Domenech, A. Crucelaegui and T. J. Leo, *ACS Sustainable Chem. Eng.*, 2022, **10**, 4300–4311.
- 21 P.-M. Heuser, D. S. Ryberg, T. Grube, M. Robinius and D. Stolten, *Int. J. Hydrogen Energy*, 2019, **44**, 12733–12747.
- 22 Y. Ishimoto, M. Voldsgård, P. Nekså, S. Roussanaly, D. Berstad and S. O. Gardarsdóttir, *Int. J. Hydrogen Energy*, 2020, **45**, 32865–32883.
- 23 M. Al-Breiki and Y. Bicer, *Energy Rep.*, 2020, **6**, 1897–1909.
- 24 Y. Sakamoto and W. Zhou, *Int. J. Energy Res.*, 2000, **24**, 549–559.
- 25 P. Preuster, A. Alekseev and P. Wasserscheid, *Annu. Rev. Chem. Biomol. Eng.*, 2017, **8**, 445–471.
- 26 H. Kim, A. Kim, M. Byun and H. Lim, *Renewable Energy*, 2021, **180**, 552–559.
- 27 C. Lang, Y. Jia and X. Yao, *Energy Storage Mater.*, 2020, **26**, 290–312.
- 28 I. A. Hassan, H. S. Ramadan, M. A. Saleh and D. Hissel, *Renewable Sustainable Energy Rev.*, 2021, **149**, 111311.
- 29 S. Saeidi, N. A. S. Amin and M. R. Rahimpour, *J. CO2 Util.*, 2014, **5**, 66–81.
- 30 E. Catizzone, C. Freda, G. Braccio, F. Frusteri and G. Bonura, *J. Energy Chem.*, 2021, **58**, 55–77.
- 31 V. Dieterich, A. Buttler, A. Hanel, H. Spliethoff and S. Fendt, *Energy Environ. Sci.*, 2020, **13**, 3207–3252.
- 32 M. Fasihi, O. Efimova and C. Breyer, *J. Cleaner Prod.*, 2019, **224**, 957–980.
- 33 D. W. Keith, G. Holmes, D. St. Angelo and K. Heidel, *Joule*, 2018, **2**, 1573–1594.
- 34 N. McQueen, K. V. Gomes, C. McCormick, K. Blumanthal, M. Pisciotta and J. Wilcox, *Prog. Energy*, 2021, **3**, 32001.
- 35 M. Erans, E. S. Sanz-Pérez, D. P. Hanak, Z. Clulow, D. M. Reiner and G. A. Mutch, *Energy Environ. Sci.*, 2022, **15**, 1360–1405.
- 36 J. Tollefson, *Nature*, 2018, **558**, 173.
- 37 International Energy Agency Greenhouse Gas R&D Programme, Global Assessment of Direct Air Capture Costs. Technical Report 2021-05, 2021, <https://ieaghg.org/publications/technical-reports/reports-list/9-technical-reports/1058-2021-05-global-assessment-of-dacs>, (accessed 27.3.2023).
- 38 J. Valentine, A. Zoelle, S. Homys, H. Mantripragada, M. Woods, N. Roy, A. Kilstofte, M. Sturdian, M. Steutermann and T. Fout, U.S. Department of Energy, Office of Scientific and Technical Information, Direct Air Capture Case Studies: Sorbent System, 2022.
- 39 M. Semmel, R. E. Ali, M. Ouda, A. Schaadt, J. Sauer and C. Hebling, in *Power to Fuel. How to Speed Up a Hydrogen Economy*, ed. G. Spazzafumo, Elsevier, 2021, pp. 123–151.
- 40 F. Pontzen, W. Liebner, V. Gronemann, M. Rothamel and B. Ahlers, *Catal. Today*, 2011, **171**, 242–250.
- 41 *Zukünftige Kraftstoffe*, ed. W. Maus, Springer Berlin Heidelberg, Berlin, Heidelberg, 2019.
- 42 Z. Azizi, M. Rezaeimanesh, T. Tohidian and M. R. Rahimpour, *Chem. Eng. Process.*, 2014, **82**, 150–172.
- 43 M. de Falco, M. Capocelli and G. Centi, *Chem. Eng. J.*, 2016, **294**, 400–409.
- 44 I. Iliuta, M. C. Iliuta and F. Larachi, *Chem. Eng. Sci.*, 2011, **66**, 2241–2251.
- 45 J. van Kampen, J. Boon, J. Vente and M. van Sint Annaland, *J. CO2 Util.*, 2020, **37**, 295–308.
- 46 J. van Kampen, J. Boon, J. Vente and M. van Sint Annaland, *React. Chem. Eng.*, 2021, **6**, 244–257.
- 47 N. Diban, A. M. Urtiaga, I. Ortiz, J. Ereñaa, J. Bilbao and A. T. Aguayo, *J. Chem. Eng.*, 2013, **234**, 140–148.
- 48 A. Ateka, J. Ereñaa, J. Bilbao and A. T. Aguayo, *Ind. Eng. Chem. Res.*, 2020, **59**, 713–722.
- 49 T. Cholewa, M. Semmel, F. Mantel, R. Güttel and O. Salem, *Chem. Eng.*, 2022, **6**, 13.



- 50 E. Pawelczyk, N. Łukasik, I. Wysocka, A. Rogala and J. Gebicki, *Energies*, 2022, **15**, 4964.
- 51 A. G. Gayubo, J. Vicente, J. Ereña, L. Oar-Arteta, M. J. Azkoiti, M. Olazar and J. Bilbao, *Appl. Catal., A*, 2014, **483**, 76–84.
- 52 K. Faungnawakij, N. Shimoda, T. Fukunaga, R. Kikuchi and K. Eguchi, *Appl. Catal., A*, 2008, **341**, 139–145.
- 53 L. Oar-Arteta, A. Remiro, J. Vicente, A. T. Aguayo, J. Bilbao and A. G. Gayubo, *Fuel Process. Technol.*, 2014, **126**, 145–154.
- 54 Z. Wang, L. Yang, R. Zhang, L. Li, Z. Cheng and Z. Zhou, *Catal. Today*, 2016, **264**, 37–43.
- 55 H. Yoshida, N. Iwasa, H. Akamatsu and M. Arai, *Int. J. Hydrogen Energy*, 2015, **40**, 5624–5627.
- 56 L. Oar-Arteta, A. Remiro, F. Epron, N. Bion, A. T. Aguayo, J. Bilbao and A. G. Gayubo, *Ind. Eng. Chem. Res.*, 2016, **55**, 3546–3555.
- 57 J.-H. Lian, H.-Y. Tan, C.-Q. Guo, Z.-D. Wang, Y. Shi, Z.-X. Lu, L.-S. Shen and C.-F. Yan, *Int. J. Hydrogen Energy*, 2020, **45**, 31523–31537.
- 58 B. Chu, D. Chang and H. Chung, *Int. J. Greenhouse Gas Control*, 2012, **10**, 46–55.
- 59 S. H. Jeon, Y. U. Choi and M. S. Kim, *Int. J. Air-Cond. Refrig.*, 2016, **24**, 1650017.
- 60 M. Al-Breiki and Y. Bicer, *Energy Convers. Manage.*, 2020, **209**, 112652.
- 61 H. Al Baroudi, A. Awoyomi, K. Patchigolla, K. Jonnalagadda and E. J. Anthony, *Appl. Energy*, 2021, **287**, 116510.
- 62 Zero emissions platform, Network technology guidance for CO<sub>2</sub> transport by ship, 2022, <https://zeroemissionsplatform.eu/wp-content/uploads/ZEP-CCSA-Guidance-Note-for-CO2-transport-by-ship-March-2022.pdf>, (accessed 27.3.2023).
- 63 A. Aspelund, M. J. Mølnvik and G. de Koeijer, *Chem. Eng. Res. Des.*, 2006, **84**, 847–855.
- 64 S. Roussanaly, H. Deng, G. Skaugen and T. Gundersen, *Energies*, 2021, **14**, 5635.
- 65 Mitsubishi Heavy Industries, Mitsubishi Shipbuilding Concludes Agreement on Construction of World's First Demonstration Test Ship for Liquefied CO<sub>2</sub> Transportation, 2022, <https://www.mhi.com/news/220202.html> (accessed 27.3.2023).
- 66 The Maritime Executive, Project to Develop CO<sub>2</sub> Carrier with Direct Injection Capabilities, 2022, <https://maritime-executive.com/article/project-to-develop-co2-carrier-with-direct-injection-capabilities> (accessed 27.3.2023).
- 67 Northern Lights, Northern Lights awards ship management contract to “K” LINE, 2022, <https://norlights.com/news/northern-lights-awards-ship-management-contract-to-k-line/>.
- 68 International Energy Agency, CO<sub>2</sub> Transport and Storage, 2022, <https://www.iea.org/reports/co2-transport-and-storage> (accessed 27.3.2023).
- 69 Committee D02 on Petroleum Products, Liquid Fuels, and Lubricants, Specification for Dimethyl Ether for Fuel Purposes, ASTM International, 2022, <https://www.astm.org/workitem-wk83482> (accessed 27.3.2023).
- 70 Air Liquide, Gas Encyclopedia Air Liquide Comparator: Material Compatibility Dimethylether & Carbon Dioxide, 2022, <https://encyclopedia.airliquide.com/compare-tool/436/336#material-compatibility> (accessed 27.3.2023).
- 71 International Energy Agency Greenhouse Gas R&D Programme, The Status and Challenges of CO<sub>2</sub> Shipping Infrastructures. Technical Report 2020-10, 2020, <https://ieaghg.org/ccs-resources/blog/new-ieaghg-report-the-status-and-challenges-of-co2-shipping-infrastructures> (accessed 27.3.2023).
- 72 X. Shi, X. Liao and Y. Li, *Renewable Energy*, 2020, **154**, 786–796.
- 73 M. A. Khan, T. Al-Attas, S. Roy, M. M. Rahman, N. Ghaffour, V. Thangadurai, S. Larter, J. Hu, P. M. Ajayan and M. G. Kibria, *Energy Environ. Sci.*, 2021, **14**, 4831–4839.
- 74 A. Panagopoulos, K.-J. Haralambous and M. Loizidou, *Sci. Total Environ.*, 2019, **693**, 133545.
- 75 H. Nazir, N. Muthuswamy, C. Louis, S. Jose, J. Prakash, M. E. Buan, C. Flox, S. Chavan, X. Shi, P. Kauranen, T. Kallio, G. Maia, K. Tammeveski, N. Lympertopoulos, E. Carcadea, E. Veziroglu, A. Iranzo and A. M. Kannan, *Int. J. Hydrogen Energy*, 2020, **45**, 20693–20708.
- 76 J.-S. Lee, A. Cherif, H.-J. Yoon, S.-K. Seo, J.-E. Bae, H.-J. Shin, C. Lee, H. Kwon and C.-J. Lee, *Renewable Sustainable Energy Rev.*, 2022, **165**, 112556.
- 77 S. F. Yin, B. Q. Xu, X. P. Zhou and C. T. Au, *Appl. Catal., A*, 2004, **277**, 1–9.
- 78 S. Schemme, J. L. Breuer, M. Köller, S. Meschede, F. Walman, R. C. Samsun, R. Peters and D. Stolten, *Int. J. Hydrogen Energy*, 2020, **45**, 5395–5414.
- 79 F. Mantei, R. E. Ali, C. Baensch, S. Voelker, P. Haltenort, J. Burger, R.-U. Dietrich, N. von der Assen, A. Schaad, J. Sauer and O. Salem, *Sustainable Energy Fuels*, 2022, **6**, 528–549.
- 80 C. Hank, A. Sternberg, N. Köppel, M. Holst, T. Smolinka, A. Schaad, C. Hebling and H.-M. Henning, *Sustainable Energy Fuels*, 2020, **4**, 2256–2273.
- 81 M. Ouda, F. Mantei, K. Hesterwerth, E. Bargiacchi, H. Klein and R. J. White, *React. Chem. Eng.*, 2018, **3**, 676–695.
- 82 International Renewable Energy Agency, Global hydrogen trade to meet the 1.5 °C climate goal: Trade outlook for 2050 and way forward, 2022, [https://www.irena.org/-/media/IRENA/Agency/Publication/2022/Jul/IRENA\\_Global\\_hydrogen\\_trade\\_part\\_1\\_2022\\_.pdf](https://www.irena.org/-/media/IRENA/Agency/Publication/2022/Jul/IRENA_Global_hydrogen_trade_part_1_2022_.pdf), (accessed 27.3.2023).
- 83 S. Banivaheb, S. Pitter, K. H. Delgado, M. Rubin, J. Sauer and R. Dittmeyer, *Chem. Ing. Tech.*, 2022, **94**, 240–255.
- 84 Linde US, Dimethyl ether, Safety Data Sheet P-4589, 2021.
- 85 B. Dutcher, M. Fan and A. G. Russell, *ACS Appl. Mater. Interfaces*, 2015, **7**, 2137–2148.

